Mathematics and Biosciences in Interaction

Managing Editor

Wolfgang Alt
Division of Theoretical Biology
Botanical Institute
University of Bonn
Kirschallee 1
D-53115 Bonn
e-mail: wolf.alt@uni-bonn.de

Editorial Board

Mathematics and Biosciences in Interaction is devoted to the publication of advanced textbooks, monographs, and multi-authored volumes on mathematical concepts in the biological sciences. It concentrates on truly interdisciplinary research presenting currently important biological fields and relevant methods being developed and refined in close relation to problems and results relevant for experimental bioscientists.

The series aims at publishing not only monographs by individual authors presenting their own results, but welcomes, in particular, volumes arising from collaborations, joint research programs or workshops. These can feature concepts and open problems as a result of such collaborative work, possibly illustrated with computer software providing statistical analyses, simulations or visualizations.

The envisaged readership includes researchers and advanced students in applied mathematics – numerical analysis as well as statistics, genetics, cell biology, neurobiology, bioinformatics, biophysics, bio(medical) engineering, biotechnology, evolution and behavioral sciences, theoretical biology, system theory.

SINGLE-CELL-BASED MODELS IN BIOLOGY AND MEDICINE

Alexander R. A. Anderson
Mark A. J. Chaplain
Katarzyna A. Rejniak

Editors

Birkhäuser
Basel • Boston • Berlin

Editors:

Dr. Alexander R.A. Anderson
Division of Mathematics
University of Dundee
23 Perth Road
Dundee DD1 4HN
UK

Dr. Katarzyna A. Rejniak
Division of Mathematics
University of Dundee
23 Perth Road
Dundee DD1 4HN
UK

Prof. Mark A.J. Chaplain
Division of Mathematics
University of Dundee
23 Perth Road
Dundee DD1 4HN
UK

Library of Congress Control Number: 2007923086

Bibliographic information published by Die Deutsche Bibliothek
Die Deutsche Bibliothek lists this publication in the Deutsche Nationalbibliografie;
detailed bibliographic data is available in the Internet at <http://dnb.ddb.de>.

ISBN 978-3-7643-8101-1 Birkhäuser Verlag AG, Basel - Boston - Berlin

Part of Springer Science+Business Media
Printed on acid-free paper produced from chlorine-free pulp. TFC ∞
Cover design: Armando Losa, graphic designer
Cover illustration: The cover image is constructed from the 3-D simulation of a growing tumour by Alexander R.A. Anderson, the 2-D simulation of an epithelial acinus by Katarzyna A. Rejniak and from a real picture of an epithelial cell by David Russell, Division of Cell and Developmental Biology, School of Life Sciences, University of Dundee.

Printed in Germany
ISBN 978-3-7643-8101-1 e-ISBN 978-3-7643-8123-3

9 8 7 6 5 4 3 2 1 www.birkhauser.ch

Contents

General Introduction ..... **vii**

I. Hybrid Multiscale Models **1**

I.1 *Alexander R.A. Anderson*
A Hybrid Multiscale Model of Tumour Invasion: Evolution and the Microenvironment **3**

I.2 *Andreas Deutsch*
Lattice-gas Cellular Automaton Modeling of Developing Cell Systems **29**

I.3 *Mark Alber, Nan Chen, Tilmann Glimm, Pavel Lushnikov*
Two-dimensional Multiscale Model of Cell Motion in a Chemotactic Field **53**

II. The Cellular Potts Model and Its Variants **77**

II.1 *James A. Glazier, Ariel Balter, Nikodem J. Popławski*
Magnetization to Morphogenesis: A Brief History of the Glazier–Graner–Hogeweg Model **79**

II.2 *Athanasius F.M. Marée, Verônica A.Grieneisen, Paulien Hogeweg*
The Cellular Potts Model and Biophysical Properties of Cells, Tissues and Morphogenesis **107**

II.3 *Nicholas J. Savill, Roeland M. H. Merks*
The Cellular Potts Model in Biomedicine **137**

II.4 *Ariel Balter, Roeland M. H. Merks, Nikodem J. Popławski, Maciej Swat, James A. Glazier*
The Glazier–Graner–Hogeweg Model: Extensions, Future Directions, and Opportunities for Further Study **151**

III. Off-lattice Cell Models **169**

III.1 *Dirk Drasdo*
Center-based Single-cell Models: An Approach to Multi-cellular Organization Based on a Conceptual Analogy to Colloidal Particles **171**

III.2 *John C. Dallon*
Models with Lattice-free Center-based Cells Interacting with Continuum Environment Variables **197**

III.3 *Timothy J. Newman*
Modeling Multicellular Structures Using the Subcellular Element Model **221**

IV. **Viscoelastic Cell Models** **241**
IV.1 *Aaron L. Fogelson*
Cell-based Models of Blood Clotting **243**
IV.2 *Eirikur Palsson*
A 3-D Deformable Ellipsoidal Cell Model with Cell Adhesion and Signaling **271**
IV.3 *Katarzyna A. Rejniak*
Modelling the Development of Complex Tissues Using Individual Viscoelastic Cells **301**

Addresses **325**

Index **329**

Colour Figures **335**

General Introduction

> *"Cell and tissue, shell and bone, leaf and flower, are so many portions of matter, and it is in obedience to the laws of physics that their particles have been moved, moulded and conformed. They are no exceptions to the rule that God always geometrizes. Their problems of form are in the first instance mathematical problems, their problems of growth are essentially physical problems, and the morphologist is, ipso facto, a student of physical science".*
> **D'Arcy W. Thompson, "On Growth and Form", 1917.**

As the great D'Arcy Thompson implicitly notes, ever since Newton and his laws of motion, continuum mathematical models have been used to describe the behaviour of "portions of matter" and "particles" in what are essentially discrete physical systems. As a result, much time and effort has been spent in justifying these continuum formulations using methods from, for example, statistical mechanics to "average out" the discreteness of the system to derive the models.

More recently, in the fields of Life and Biomedical Sciences, the past 10–15 years have witnessed enormous advances in our understanding of the molecular basis of cell structure and function. The spectacular success of the human genome project and the consequent burgeoning interest in the related field of proteomics have brought these achievements to the attention not only of the scientific community but also the general public. Biochemists and cell biologists have made similarly impressive strides in elucidating the mechanisms mediating cell signalling and its consequences for the control of cell proliferation, motility and gene expression. It is, however, abundantly clear that reductionist logic using this impressive "sub-cell-level" information base is not sufficient to deduce an understanding of phenomena operating at higher levels of biological organisation. Employing a literary analogy, the vast "omic" databases of catalogued genes and proteins, taken together with our growing understanding of the inner workings of individual cells, provide a "dictionary" and a "grammatical syntax" required for the next great challenge i.e. understanding the "sentences" and "paragraphs" characteristic of emergent higher-level cellular phenomena.

With recent advances in applied mathematics, numerical analysis and computational techniques, multiscale mathematical modelling is now being brought to bear on many challenging problems in the Life and Biomedical Sciences, particularly where cellular systems are concerned. Indeed, in a somewhat ironic twist due to the enhancement of computational processing power, continuum models of discrete systems are frequently approximated by discrete models which can be solved computationally. As computers have become more powerful, there has been renewed interest in mathematical models of biological systems maintaining a discrete formulation from the outset.

In the words of D'Arcy Thompson yet again:
"I know that in the study of material things, number, order and position are the threefold clues to exact knowledge; that these three, in the mathematician's hands, furnish the 'first outlines for a sketch of the Universe'."

The development of new mathematical techniques and their application to biological systems will no doubt be beneficial for "both sides". In the words of David Hilbert, applying mathematics to specific problems is the best way to further develop and deepen one's understanding of the mathematics:
"He who seeks for methods without having a definite problem in mind seeks in the most part in vain. The further a mathematical theory is developed, the more harmoniously and uniformly does its construction proceed, and unsuspected relations are disclosed between hitherto separated branches of the science."

With regard to the specific content of this book, applied mathematics and modelling is sure to benefit from continued interaction with experimentalists working on cellular systems. In recent years many different single-cell-based models have been developed and applied successfully to various biological and medical problems. These models employ very different computational approaches: Monte-Carlo simulations, energy minimisation techniques, volume conservation laws, solutions of the equations of motion for each individual cell or for each point on a cell membrane. They also differ in the level of detail that defines the cell structure and subsequently differ in the number of individual cells that the model can incorporate. The principal aim of this book is to gather together a collection of different mathematical and computational single-cell-based models and present their applications in biology and medicine. This book is addressed equally to students starting their research in the field of mathematical biology and to scientists already modelling multi-cellular processes. Therefore, each chapter contains a detailed description of a particular model and an extensive review of suitable biological and medical applications. This book is also accompanied by a DVD containing simulation movies of all presented models and applications.

What is certain at the present time, and for the foreseeable future, is that interdisciplinary activity between biology and mathematics, with a genuine dialogue between the participating partners, may be viewed as the most fruitful way to advance scientific understanding in both subjects. These are genuinely exciting times to be involved in the subject. Over a century later, the words of David Hilbert are particularly apposite and have a powerful resonance for the application of discrete modelling techniques in the area of cell biology:

"Who of us would not be glad to lift the veil behind which the future lies hidden; to cast a glance at the next advances of our science and at the secrets of its development during future centuries? What particular goals will there be toward which the leading mathematical spirits of coming generations will strive? What new methods and new facts in the wide and rich field of mathematical thought will the new centuries disclose?"

D. Hilbert, opening of his speech to the 1900 Mathematics Congress in Paris.

Finally, the editors of this book would like to express their sincere thanks to all the contributors.

Dundee, February 2007

Single-Cell-Based Models in Biology and Medicine
ed. by A.R.A. Anderson, M.A.J. Chaplain, K.A. Rejniak
Mathematics and Biosciences in Interaction, 1

I. Hybrid Multiscale Models

General Introduction

Many mathematical models of biological process that consider space explicitly, fall into one of two categories: (i) continuum population models or (ii) discrete individual based models. Discrete, stochastic interactions between individual organisms cannot be captured by the continuum approach and likewise global population interactions cannot be captured by the discrete approach. In recent years a third category of models has emerged: hybrid models which allow modellers to exploit the advantages of both continuum and discrete models. The advantages of using such hybrid approaches are clear when dealing with organisms that involve processes at different scales e.g. a cell migrating up a chemical gradient. Such hybrid models are by definition multiscale as they already model interactions between variables that occur on different scales (e.g. micro and macro scale). In this initial section of the book we examine a range of grid based hybrid approaches.

The first chapter from A. Anderson, A Hybrid Multiscale Model of Tumour Invasion: Evolution and Microenvironment, discusses the Hybrid Discrete-Continuum (HDC) technique that uses an initial continuum model as the basis for the derivation of the HDC model. This allows the tumour cells to be represented as discrete individuals with an internal life cycle that describes how they interact with continuum microenvironmental variables and one another. In addition, all cells are assigned phenotypic traits that define their behaviour which, via mitosis, are allowed to mutate using two different mutation algorithms.

In the following chapter from A. Deutsch, Lattice-gas Cellular Automaton Modelling of Developing Cell Systems, in which he defines this cellular automaton approach and examines both via simulation and analysis its dynamical properties. By applying the Boltzmann equations derived from the lattice-gas cellular automata (LGCA) the role of cell-based instabilities is examined. Application of LGCA to both chemotaxis and adhesion is considered.

In third chapter M. Alber presents a Two-dimensional Multiscale Model of Cell Motion in a Chemotactic Field. Focusing on the discrete cellular potts model (CPM) and, by means of a limiting procedure, the equivalent continuous model. In particular, the connection between a CPM of a cell reacting to a chemical field, and a Fokker-Planck equation for the cell probability density function is discussed. The Fokker-Planck equation is then reduced to the classical Keller-Segel equation which is then compared numerically to CPM simulations and shows good agreement.

Single-Cell-Based Models in Biology and Medicine
ed. by A.R.A. Anderson, M.A.J. Chaplain, K.A. Rejniak
Mathematics and Biosciences in Interaction, 3–28

I.1 A Hybrid Multiscale Model of Solid Tumour Growth and Invasion: Evolution and the Microenvironment

Alexander R. A. Anderson

Abstract. Cancer is a complex, multiscale process, in which genetic mutations occurring at a subcellular level manifest themselves as functional changes at the cellular and tissue scale. The importance of tumour cell/microenvironment interactions is currently of great interest to both the biological and the modelling communities. In this chapter we present a hybrid discrete-continuum (HDC) mathematical model of tumour invasion that considers the tumour as a collection of many individual cancer cells that interact with and modify the environment through which they grow and migrate. The HDC model we develop focuses on four key variables implicated in the invasion process: tumour cells, host tissue (extracellular matrix), matrix-degradative enzymes and oxygen. The model is considered to be hybrid since the latter 3 variables are continuous (i.e. concentrations) and the tumour cells are discrete (i.e. individuals). We shall examine how individual-based cell interactions (with one another and the microenvironment) can affect the tumour morphology. We will also discuss the evolutionary influence that the microenvironment has upon the tumours genetic makeup. The HDC model focuses on the microscale (individual cell) level to produce computational simulations of tumour at the tissue scale. As we shall discuss, this technique, developed in previous models of nematode migration and angiogenesis, is intrinsically multiscale and can easily incorporate a range of scales i.e. genetic, sub-cellular, cellular and tissue.

1. Tumour Invasion

The development of a primary solid tumour (e.g. a carcinoma) begins with a single normal cell becoming transformed as a result of mutations in certain key genes. This transformed cell differs from a normal one in several ways, one of the most notable being its escape from the body's homeostatic mechanisms, leading to inappropriate proliferation. An individual tumour cell has the potential, over successive divisions, to develop into a cluster (or nodule) of tumour cells. Further growth and

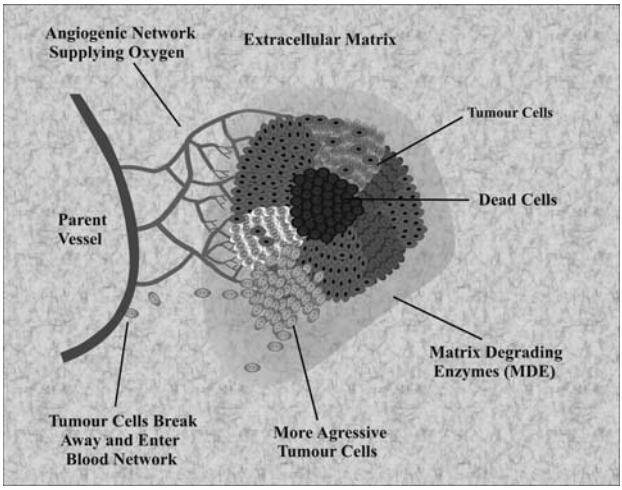

FIGURE 1. Schematic diagram showing the key variables involved in solid tumour growth: Tumour cells, extracellular matrix, matrix degrading enzyme and oxygen. The tumour contains a heterogeneous population of cells with varying degrees of aggressiveness.

proliferation leads to the development of an avascular tumour consisting of approximately 10^6 cells. Since the tumour is dependent on diffusion as the only means of receiving nutrients and removing waste products its growth is limited. For any further development to occur the tumour must initiate angiogenesis–the recruitment of blood vessels from a pre-existing vascular network. Once angiogenesis is complete, the perfused vascular network can supply the tumour with the nutrients it needs to grow further. There is also now the possibility of tumour cells finding their way into the circulatory system (via the vascular network) and being deposited at distant sites in the body, resulting in metastases (secondary tumours). Clearly angiogenesis, the process which results in the tumour having a vascular network, is a key process for metastatic invasion (see Fig.1).

Central to the invasive process are the molecules that facilitate interactions between cells and between cells and the *extracellular matrix* (ECM), known as cell adhesion molecules. A common feature of cell adhesion molecules is their ability to function as a molecular bridge between an external ligand and the cytoskeleton within the cell [13]. Over the past few years, it has become clear that receptors that mediate cell adhesion do not just affect cell migration, since occupancy of cell-surface receptors results in the initiation of signal-transduction pathways that regulate many aspects of cell function [13, 29] including transcription, proliferation, differentiation, cytoskeletal organisation and receptor activation [16].

A crucial part of the invasive/metastatic process is the ability of the cancer cells to degrade the surrounding tissue or *extracellular matrix* (ECM) [46]. This is a complex mixture of macromolecules (MM), some of which, like the collagens, play

a structural role and others (such as laminin, fibronectin and vitronectin) are important for cell adhesion, spreading and motility. We note that all of these macromolecules are *bound* within the tissue, i.e. they are non-diffusible. The ECM can also sequester growth factors and itself be degraded to release fragments which can have growth-promoting activity. Thus, while the ECM may have to be physically removed in order to allow a tumour to spread, its degradation may, in addition, have biological effects on tumour cells.

A number of *matrix degradative enzymes* (MDEs) such as the *plasminogen activator* (PA) system and the large family of *matrix metalloproteinases* (MMPs) have been described [50] and both of these have been repeatedly implicated in tumour invasion and metastasis. In addition to opening migratory pathways, MDEs can alter cell adhesion properties regulated through several classes of cell surface receptors. These receptors, including cadherins, CD-44, integrins, and receptors for fibronectin, laminin, and vitronectin, negatively regulate cell motility and growth through cell-cell and cell-matrix interactions [46]. Therefore, proteolytic degradation of receptor and/or ECM components could release tumour cells from these constraints. Recent studies have shown that CD-44 mediates the attachment of cells to various MM, in fact invasion of human glioma cells has been inhibited by antibodies against CD-44 [33]. Molecules which facilitate interactions between cells and between cells and the ECM, known as cell adhesion molecules, are now thought to be central to the invasive process [29]. Therefore it is important for any model that considers tumour invasion to include both cell-cell and cell-matrix interactions.

Tumour heterogeneity at the genetic level is well known and the so called "Guardian of the Genome", the p53 gene is widely considered as a precursor to much wider genetic variation [34]. The p53 protein links three cellular functions: proliferation, death and DNA repair. In normal cells, p53 blocks proliferation and enables damaged DNA to be repaired. If DNA repair is incomplete, apoptosis is initiated and the cell dies. Loss of p53 function (e.g. through mutation) allows for the propagation of damaged DNA to daughter cells [34]. Once the p53 mutation occurs many more mutations can easily accrue, these changes in the tumour cell genotype ultimately express themselves as behavioural changes in cell phenotype. As a step towards the inclusion of true tumour heterogeneity we shall consider a tumour that has phenotypic heterogeneity. The tumour cell phenotype will be defined here in terms of the level of a cell's aggressiveness, i.e. a combination of its cell-cell adhesiveness, proliferation, degradation and migration rates (further details will be discussed below).

The importance of the tumour microenvironment is currently of great interest to both the biological and the modelling communities. In particular, both the immediate microenvironment (cell-cell or cell-matrix interactions) and the extended microenvironment (e.g. vascular bed) are thought to play crucial roles in both tumour progression and suppression (see the recent series of papers in Nature Reviews Cancer for further detail, [2, 11, 39]). Aggressive tumours are often described as having an invasive phenotype, characterised by fingering margins as opposed

to more benign tumours which are characterised by smooth non-invasive margins. Recently it has been shown that not only can the microevironment promote tumour progression but it can also drive the invasive tumour phenotype. The work of Weaver [40] focuses on the impact of tissue tension in driving the invasive phenotype and clearly correlates higher tension in the tissue (a harsher environment) with an invasive phenotype. Similarly Pennacchietti [41] has shown a relationship between a hypoxic tumour microenvironment (again a harsher environment) and the invasive phenotype.

2. Hybrid Discrete-Continuum Technique

When deciding which model should be used, the number and scale of the organisms being modelled is important and the manner in which the organisms interact with their environment and each other is also important. Discrete, stochastic interactions between organisms cannot be captured by the continuum approach and likewise global population interactions cannot be captured by the discrete approach. Therefore the most appropriate modelling technique depends on both the number of organisms and scale at which they are being studied.

Over the last ten years or so many mathematical models of tumour growth, both temporal and spatio-temporal, have appeared in the research literature (see [20] for a review of many of these and for a more recent review see [10]). Deterministic reaction-diffusion equations have been used to model the spatial spread of tumours both at an early stage in its growth [44, 51] and at the later invasive stage [37, 26, 42, 5, 47, 48]. Typical solutions observed in all these models [37, 26, 42, 14] appear as invading travelling waves of cancer cells. Whilst these models are able to capture the tumour structure at the tissue level, they fail to describe the tumour at the cellular level and subsequently the subcellular level. On the other hand, cellular automata models provide such a description and allow a more realistic stochastic approach at both the cellular ([32, 45, 43, 7, 31, 21]) and subcellular levels [22, 23].

The model presented here is of a different type: we classify this as "Hybrid", since a continuum deterministic model (based on a system of reaction-diffusion-chemotaxis equations) controls the chemical/ECM dynamics and a discrete cellular automata like model (based on a biased random-walk model) controls the cell migration and interaction. Initially we define a system of coupled nonlinear partial differential equations to model tumour invasion of surrounding tissue. We then use a discretised form of the partial differential equation governing cell migration as the basis for the hybrid discrete-continuum model. This then enables specific cell properties to be modelled at the level of the individual cell, we shall consider proliferation, death, cell-cell adhesion, mutation, and production/degradation at the individual cell level. The crucial point of this technique is that it allows cells to be treated as discrete individuals and the cell processes to be modelled at the level of the cell whilst allowing the the chemicals/ECM to be treated as continuous. A

detailed discussion on the types of system that this technique is applicable to is given in [6]. Applications of the technique can be found in [3]–[9].

In the last few years there has been a rapid development in such hybrid models in application to tumour growth. The work of Deutsch [36], Deisboeck [52] and Alarcon [1] have all coupled individual tumour cells with continuous chemical dynamics. However, non of these has explicitly modelled the direct impact of the microenvironment upon both the tumour cell population at the phenotype scale and the resulting changes in tumour geometry at the organ scale.

The aim of this chapter is to show how the tumour microenvironment impacts directly upon both tumour morphology and tumour heterogeneity. By using a combination of different microenvironments (e.g. homogeneous, heterogeneous tissue, low/high nutrient concentration) with different mutation algorithms (i.e. linear or random) we will show that how aggressiveness of a tumour is directly correlated with the microenvironment in which it grows.

3. The Continuum Model

We will base our mathematical model on the growth of a generic three dimensional solid tumour. We will model both the full three dimensional tumour volume and a two dimensional slice through this, one cell diameter thick. We choose to focus on four key variables involved in tumour invasion, thereby producing a minimal model, namely; tumour cell density (denoted by n), MDE concentration (denoted by m), MM concentration (denoted by f) and oxygen concentration (denoted by c), see Fig.1. Initially we define a system of coupled nonlinear partial differential equations to model tumour invasion of surrounding tissue and use these as the basis for the *Hybrid Discrete-Continuum* (HDC) technique.

The complete system of equations describing the interactions of the tumour cells, MM, MDEs and oxygen is

$$\begin{aligned}
\frac{\partial n}{\partial t} &= \overbrace{D_n \nabla^2 n}^{random\ motility} - \overbrace{\chi \nabla \cdot (n \nabla f)}^{haptotaxis}, \\
\frac{\partial f}{\partial t} &= - \overbrace{\delta m f}^{degradation}, \\
\frac{\partial m}{\partial t} &= \overbrace{D_m \nabla^2 m}^{diffusion} + \overbrace{\mu n}^{production} - \overbrace{\lambda m}^{decay}, \\
\frac{\partial c}{\partial t} &= \overbrace{D_c \nabla^2 c}^{diffusion} + \overbrace{\beta f}^{production} - \overbrace{\gamma n}^{uptake} - \overbrace{\alpha c}^{decay},
\end{aligned} \tag{1}$$

were D_n, D_m and D_c are the tumour cell, MDE and oxygen diffusion coefficients respectively, χ the haptotaxis coefficient and δ, μ, λ, β, γ and α are positive constants. We should also note that cell-matrix adhesion is modelled here by the use of haptotaxis in the cell equation i.e. directed movement up gradients of MM. Therefore χ maybe considered as relating to the strength of the cell-matrix adhesion.

Since this model has already been published [8, 9] we will not discuss its derivation here. However, some explanation should be given to the manner in which oxygen is modelled. Oxygen is assumed to diffuse into the MM, decay naturally and be consumed by the tumour. For simplicity oxygen production is proportional to the MM density, this might be considered as modelling the pre-existing blood supply. This is a crude way of modelling an angiogenic oxygen supply, see Anderson & Chaplain [4] for a more appropriate way of modelling the angiogenic network. Since oxygen production is directly proportional to MM density, as the MM is degraded the oxygen production will drop.

The above system of equations can be used to model both two- and three-dimensional tumour invasion. In 2D the system is considered to hold on a square of tissue Ω of length L, while in 3D it holds on a cube of tissue Ω of side L both with appropriate initial conditions for each variable. We assume that the MM, oxygen, tumour cells and consequently the MDEs, remain within the domain of tissue under consideration and therefore no-flux boundary conditions are imposed on $\partial\Omega$, the boundary of Ω.

3.1. Non-dimensionalisation and Parameterisation

In order to use realistic parameter values we first of all non-dimensionalise the equations in the standard way. We rescale distance with an appropriate length scale L (e.g. the maximum invasion distance of the cancer cells at this early stage of invasion, approximately 1cm), time with τ (e.g. the average time take for mitosis to occur, approximately $8-24$hrs [15], tumour cell density with n_0, ECM density with f_0, MDE concentration m_0 and oxygen concentration with c_0 (where n_0, f_0, m_0, c_0 are appropriate reference variables). Therefore setting

$$\tilde{n} = \frac{n}{n_0},\ \tilde{f} = \frac{f}{f_0},\ \tilde{m} = \frac{m}{m_0},\ \tilde{c} = \frac{c}{c_0},\ \tilde{\mathbf{x}} = \frac{\mathbf{x}}{L},\ \tilde{t} = \frac{t}{\tau}$$

in Eq.(1) and dropping the tildes for notational convenience, we obtain the scaled system of equations:

$$\begin{aligned}
\frac{\partial n}{\partial t} &= \overbrace{d_n\nabla^2 n}^{random\ motility} - \overbrace{\rho\nabla\cdot(n\nabla f)}^{haptotaxis},\\
\frac{\partial f}{\partial t} &= -\overbrace{\eta m f}^{degradation},\\
\frac{\partial m}{\partial t} &= \overbrace{d_m\nabla^2 m}^{diffusion} + \overbrace{\kappa n}^{production} - \overbrace{\sigma m}^{decay},\\
\frac{\partial c}{\partial t} &= \overbrace{d_c\nabla^2 c}^{diffusion} + \overbrace{\nu f}^{production} - \overbrace{\omega n}^{uptake} - \overbrace{\phi c}^{decay},
\end{aligned} \tag{2}$$

where $d_n = \tau D_n/L^2,\ \rho = \tau\chi f_0/L^2,\ \eta = \tau m_0\delta,\ d_m = \tau D_m/L^2,\ \kappa = \tau\mu n_0/m_0,\ \sigma = \tau\lambda,\ d_c = \tau D_c/L^2,\ \nu = \tau f_0\beta/c_0,\ \omega = \tau n_0\gamma/c_0,\ \phi = \tau\alpha.$

The cell cycle time depends on the specific tumour under consideration, as a rough guide we take $\tau = 16$hrs, halfway between $8 - 24$hrs [15]. The cell motility parameter $D_n \sim 10^{-9}\text{cm}^2\text{s}^{-1}$ was estimated from available experimental evidence [12]. Tumour cell diameters again will vary depending on the type of tumour being considered but are in the range $10 - 100\mu m$ [35] with an approximate volume of $10^{-9}cm^3 - 3 \times 10^{-8}cm^3$, [25, 17]. We will assume that a tumour cell has the volume $1.5 \times 10^{-8}cm^3$ and therefore take $n_0 = 6.7 \times 10^7$ cells$/cm^3$. The haptotactic parameter $\chi \sim 2600\text{cm}^2\text{s}^{-1}\text{M}^{-1}$ was estimated to be in line with that calculated in Anderson *et al.* [4] and the parameter $f_0 \sim 10^{-8} - 10^{-11}$M was taken from the experiments of Terranova *et al.* [49]. We took D_m to be $10^{-9}\text{cm}^2\text{s}^{-1}$, which is perhaps small for a diffusing chemical, but recent experimental evidence implies that it is in fact a combination of the MDE and MM which results in degradation of the MM and that this bound chemical diffuses very little [28]. An *in vivo* estimate for the MDE concentration m_0 is somewhat difficult to obtain since there is currently no published value (that we are aware of). Plasma levels of specific MDEs have been measured (e.g. MMP-2, [53]) and are approximately $130ng/ml$ with further increases observed in patients with cancer [30]. How this relates to the MDE concentration within the ECM is not clear, we have therefore left this parameter undefined. Estimates for the kinetic parameters μ, λ, δ were not available since these are very difficult to obtain experimentally, we therefore use the values of [4]. Oxygen is known to diffuse through water at a rate of $D_c = 10^{-5}\text{cm}^2\text{s}^{-1}$ and cells consume oxygen at a rate of $6.25 \times 10^{-17}\text{Mcell}^{-1}\text{s}^{-1}$[17]. The background oxygen concentration within the tissue was somewhat difficult to estimate, we shall use $c_0 = 6.7 \times 10^{-6}\text{MO}_2\text{cm}^{-3}$ as discussed in [8].

4. The Discrete Model

Now that we have defined the continuum model of tumour invasion we can implement the hybrid discrete-continuum technique (see [3]–[9]) which will allow us to follow the paths of individual tumour cells. This first involves discretising (using standard finite-difference methods) the system of partial differential equations (2). We then use the resulting coefficients of the finite-difference stencil to generate the probabilities of movement of an individual cell in response to its local milieu (see Appendix of [5] for the full discrete system). Once the movement probabilities have been defined, both two and three dimensions will be discussed, we then consider the specific individual based processes that we will incorporate into the model.

4.1. Two Dimensions

As an illustration of the technique we only consider the tumour cell equation and discretise Eq.(2) in two spatial dimensions using central finite difference approximations to obtain the following,

$$n_{i,j}^{q+1} = n_{i,j}^q P_0 + n_{i+1,j}^q P_1 + n_{i-1,j}^q P_2 + n_{i,j+1}^q P_3 + n_{i,j-1}^q P_4. \tag{3}$$

where the subscripts specify the location on the grid and the superscripts the time steps. That is $x = ih$, $y = jh$ and $t = qk$ where i, j, k, q and h are positive parameters. In a numerical simulation of the continuous model Eq.(2), the purpose of the discrete equation Eq.(3) is to determine the tumour cell density at grid position (i, j), and time $q + 1$, by averaging the density of the four surrounding neighbours at the previous time step q. However, for the HDC technique, we will use the five coefficients P_0 to P_4 from Eq.(3) to generate the motion of an individual tumour cell. The central assumption of the HDC technique is that these five coefficients can be thought of as being proportional to the probabilities of a cell being stationary (P_0) or moving west (P_1), east (P_2), south (P_3) or north (P_4) one grid point (h) at each time step (k).

The coefficient P_0, which is proportional to the probability of no movement, has the form,

$$P_0 = 1 - \frac{4kD_n}{h^2} - \frac{k\rho}{h^2}\left(f^q_{i+1,j} + f^q_{i-1,j} - 4f^q_{i,j} + f^q_{i,j+1} + f^q_{i,j-1}\right), \tag{4}$$

and the coefficients P_1 ,P_2 ,P_3 and P_4, which are proportional to the probabilities of moving west, east, south and north respectively, have the forms,

$$\begin{aligned} P_1 &= \frac{kD}{h^2} - \frac{k\rho}{4h^2}\left[f^q_{i+1,j} - f^q_{i-1,j}\right], \\ P_2 &= \frac{kD}{h^2} + \frac{k\rho}{4h^2}\left[f^q_{i+1,j} - f^q_{i-1,j}\right], \\ P_3 &= \frac{kD}{h^2} - \frac{k\rho}{4h^2}\left[f^q_{i,j+1} - f^q_{i,j-1}\right], \\ P_4 &= \frac{kD}{h^2} + \frac{k\rho}{4h^2}\left[f^q_{i,j+1} - f^q_{i,j-1}\right], \end{aligned} \tag{5}$$

where the subscripts specify the location on the grid and the superscripts the time steps, all parameters are positive and are as discussed above. From these we see that if there were no MM the values of P_1 to P_4 would be equal, with P_0 smaller (or larger, depending on the precise values chosen for the space and time steps) i.e. there is no bias in any one direction and the tumour cell is less (more) likely to be stationary - approximating an unbiased random walk. However, if there are gradients in the MM, haptotaxis contributes to the migration process and the coefficients P_1 to P_4 will become biased towards the direction of increased MM concentration. The equation P_0 represents the probability of a cell being stationary and takes into account the situation when a single cell does not experience a gradient between neighboring points because they contain equal concentrations of MM; if neighbouring points contain higher (lower) MM concentrations, the probability of being stationary is diminished (increased) by the sign and magnitude of the term $\left(f^q_{i+1,j} + f^q_{i-1,j} - 4f^q_{i,j} + f^q_{i,j+1} + f^q_{i,j-1}\right)$ see Anderson [8] for a full derivation. The motion of an individual cell is therefore governed by its interactions with the matrix macromolecules in its local environment. Of course the motion will also be modified by interactions with other tumour cells.

4.2. Three Dimensions

This technique can easily be extended to three dimensions by employing the same standard finite-difference methods but this time we use the resulting coefficients of the seven-point finite-difference stencil to generate the probabilities of movement of an individual cell in response to its environment. Again, we only consider the discrete tumour cell equation:

$$\begin{aligned} n^{q+1}_{i,j,w} = n^q_{i,j,w}P_0 &+ n^q_{i+1,j,w}P_1 + n^q_{i-1,j,w}P_2 + n^q_{i,j+1,w}P_3 \\ &+ n^q_{i,j-1,w}P_4 + n^q_{i,j,w+1}P_5 + n^q_{i,j,w-1}P_6, \end{aligned} \tag{6}$$

The coefficient P_0, which is proportional to the probability of no movement, has the form,

$$\begin{aligned} P_0 = 1 - \frac{6kD_n}{h^2} - \frac{k\rho}{h^2}(f^q_{i+1,j,w} &+ f^q_{i-1,j,w} + f^q_{i,j,w+1} - 6f^q_{i,j,w} \\ &+ f_{i,j,w-1} + f^q_{i,j+1,w} + f^q_{i,j-1,w}), \end{aligned} \tag{7}$$

and the coefficients P_1, P_2, P_3, P_4, P_5, P_6 which are proportional to the probabilities of an individual tumour cell moving west, east, south, north, down, or up respectively, have the forms,

$$\begin{aligned} P_1 &= \frac{kD}{h^2} - \frac{k\rho}{4h^2}\left[f^q_{i+1,j,w} - f^q_{i-1,j,w}\right], \\ P_2 &= \frac{kD}{h^2} + \frac{k\rho}{4h^2}\left[f^q_{i+1,j,w} - f^q_{i-1,j,w}\right], \\ P_3 &= \frac{kD}{h^2} - \frac{k\rho}{4h^2}\left[f^q_{i,j+1,w} - f^q_{i,j-1,w}\right], \\ P_4 &= \frac{kD}{h^2} + \frac{k\rho}{4h^2}\left[f^q_{i,j+1,w} - f^q_{i,j-1,w}\right], \\ P_5 &= \frac{kD}{h^2} - \frac{k\rho}{4h^2}\left[f^q_{i,j,w+1} - f^q_{i,j,w-1}\right], \\ P_6 &= \frac{kD}{h^2} + \frac{k\rho}{4h^2}\left[f^q_{i,j,w+1} - f^q_{i,j,w-1}\right], \end{aligned} \tag{8}$$

where the subscripts specify the location on the grid and the superscripts the time steps. That is $x = ih$, $y = jh$, $z = wh$ and $t = qk$ where i, j, w, k, q and h are positive parameters.

These seven probabilities P_0 to P_6 from Eq.(7) and Eq.(8) are used to generate the motion of each tumour cell in three spatial dimensions. As with the two dimensional probabilities, they are functions of the local MM concentration and therefore the motion of an individual cell is governed by its interactions with the the local MM environment and with one another.

4.3. Individual-Based Processes

Since we model individual tumour cells we have the ability to incorporate individual based processes. We now discuss in detail the processes each tumour cell will experience as it migrates through the MM field, driven by either the two-dimensional or three-dimensional movement probabilities defined in the above sections. As a step towards the inclusion of true tumour heterogeneity we shall consider a tumour that has phenotypic heterogeneity. The tumour cell phenotype

will be defined here by the level of the cell's aggressiveness, i.e. a combination of its cell-cell adhesiveness, proliferation, degradation and migration rates (see cell phenotype paragraph below).

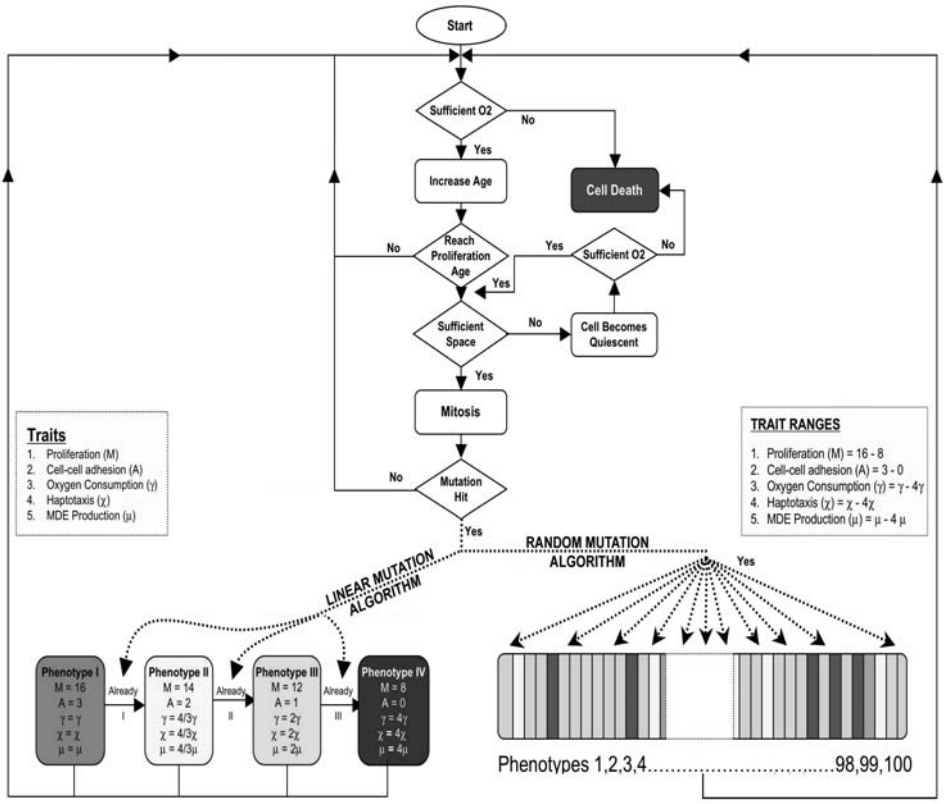

FIGURE 2. Flowchart of the tumour cell life-cycle within the hybrid discrete-continuum simulation. At the point where a mutation can occur, either follow the linear mutation algorithm only, or the random mutation algorithm only. See text for further details.

Life Cycle

Fig.2 shows a flowchart of a tumour cell's "life-cycle" within the hybrid discrete-continuum simulation. At each time step a tumour cell will initially check if it can move with regards to cell-cell adhesion restrictions (see the next paragraph for criteria), if it can, then the movement probabilities (above) are calculated and the cell is moved. A check is then made to see if there is sufficient oxygen for the cell to survive (see the paragraph on necrosis) if not, the cell dies. If there is sufficient oxygen, the cells age is increased and a check is performed to see if it has reached proliferation age. If it has not reached this age then it starts the whole loop again.

If proliferation age has been reached then a check is made to see if the criteria for proliferation are satisfied (see proliferation paragraph for details). If proliferation criteria are not met then the cell becomes quiescent. If they are satisfied then we check to see if this mitosis results in a mutation hit. All mutations in a particular simulation will be assumed to occur in either a Linear (Fig.2, left) or Random (Fig.2, right) manner (see mutation paragraph for details). This whole process is repeated at each time step of the simulation.

Cell-Cell Adhesion
To model cell-cell adhesion explicitly we assume each cell has its own internal adhesion value (A_i, see Table 1) i.e. the number of neighbours that it will preferentially adhere to. We therefore examine the number of external neighbours each cell has (A_e) and if $A_e \geq A_i$ then the cell is allowed to migrate, otherwise it remains stationary. Whilst this is a somewhat crude way of modelling cell adhesion, it does capture some features of cell-cell adhesion e.g. certain cells are more likely to bind to others and in so doing restrict their own ability to migrate.

Necrosis
For a tumour cell to survive it requires sufficient oxygen, since some tumour cells have been found to survive in very poorly oxygenated environments, we make the assumption that the concentration has to drop to 0.05 non-dimensional units (where 1 would be the initial concentration) for cell death to occur. This assumption is also applied to quiescent tumour cells. The space that dead cells occupy becomes available to new cells as soon as they die.

Proliferation
In our model we assume that each individual cell has the capacity for proliferation and will produce two daughter cells, provided: (i) the parent cell has reached maturity (Mhrs, see Table 1) and (ii) there is sufficient space surrounding the parent cell for the two new daughter cells to occupy. In order to satisfy condition (ii), we assumed that one daughter cell replaces the parent cell and the other daughter cell will move to any one of the parent cell's four orthogonal neighbours that is

Phenotype	Proliferation Age M	O_2 Uptake	MDE Production	A_i	Haptotaxis
Linear I (orange)	16hrs	ω	κ	3	ρ
Linear II (green)	14hrs	$4/3\omega$	$4/3\kappa$	2	$4/3\rho$
Linear III (cyan)	12hrs	2ω	2κ	1	2ρ
Linear IV (blue)	8hrs	4ω	4κ	0	4ρ
Random	$8-16$hrs	$\omega-4\omega$	$\kappa-4\kappa$	$0-3$	$\rho-4\rho$

TABLE 1. Parameter values for each of the four different Phenotypes in the linear mutation algorithm as well as the ranges for each trait in the random mutation algorithm. Colours are used to identify the different phenotypes in the simulation results.

empty. If more than one of the neighbouring grid points is empty then the new cell position is chosen randomly from these points. If no empty neighbours exist then the cell becomes quiescent and proliferation is delayed until space becomes available. We therefore do not consider the possibility that cells may push neighbouring cells to create free space in which to proliferate. Quiescent tumour cells are assumed to consume half the oxygen of tumour cells [24].

Production/Degradation/Diffusion
Since we are modelling individual tumour cells we must consider MDE production at the level of a single cell. In the continuum model Eq.(2) we have MDE production as being proportional to the tumour cell density. Now MDE is only produced at a grid point if a tumour cell is occupying that grid point. Since we have no precise parameter estimates for this production rate, we take $n = 1$ in the discrete form of the MDE equation when a tumour cell is occupying the current location and take $n = 0$ otherwise. Similarly for O_2 uptake, we take $n = 1$ (since ω is scaled as per cell) in the discrete form of the oxygen equation when a cell is consuming oxygen at the current location and $n = 0$ otherwise. Since the tumour cells occupy physical space within the ECM we should consider how this might impact upon oxygen diffusion. It seems logical that oxygen diffusion will be reduced as the space occupied by the tumour increases, this is consistent with tumour spheroid results i.e. as the spheroid diameter increases the necrotic region also increases. To model this at the individual level, we assume that oxygen diffusion decreases at the grid point a tumour cell occupies i.e. the oxygen diffusion rate at that grid point will be $d_{c_{cell}} < d_c$.

Cell Phenotype
Each cell has predefined phenotypic traits that describe its behaviour. We have chosen these phenotypes based on the current views of the invasive phenotype [27]. Table 1 shows the different values each phenotype takes and clearly type IV is the most aggressive, having the shortest proliferation age, consuming the most O_2, producing the most MDE, having the largest haptotaxis coefficient and requiring no neighbours for migration. We have chosen to correlate tumour cell aggressiveness with proliferation age, O_2 uptake, MDE production, cell-cell adhesion coefficient and haptotaxis coefficient. We assume that O_2 uptake, MDE production and haptotaxis coefficients all increase and the proliferation age and adhesion coefficients decrease as the tumour cell phenotype becomes increasingly aggressive.

Mutation Algorithm
Since the manner in which tumour cell mutation is modelled will directly impact on the cell life-cycle flowchart and consequently the resulting tumour population heterogeneity, we will consider two different mutation algorithms: (a) Linear (Fig.2, left) and (b) Random (Fig.2, right). (a) In the linear algorithm, all cells are initially assigned the values of phenotype I (as defined in Table 1, the least aggressive). For each subsequent proliferation there is a small probability (P_{mutat}) of further mutations occurring which will lead to phenotype II and so on in a linear fashion.

All mutations in the linear algorithm are assumed to be irreversible. (b) The random mutation algorithm on the other hand does allow mutations to be reversible, albeit within the constraints of the 100 randomly pre-defined phenotypes, as each of these phenotypes has an equal probability of being selected (see Fig.2, right). Each of the 100 phenotypes will have a randomly selected proliferation age, O_2 consumption, MDE production, haptotaxis coefficient and adhesion value all within the ranges of values defined in Table 1. Each initial cell is assigned the values of one of the 100 randomly selected phenotypes and for each subsequent proliferation there is a small probability (P_{mutat}) of further mutations occurring which will lead to another randomly selected phenotype and so on.

4.4. Simulation Process for the Hybrid Discrete-Continuum Model

Each time step of the simulation process involves solving the discrete form of the system Eq.(2) numerically to generate the five coefficients P_0 to P_4, Eqs.(4)–(5), in two dimensions (in three dimensions we generate the seven coefficients P_0 to P_6 using Eqs.(7)–(8)). We then normalise these coefficients to obtain the corresponding final probabilities of motion, where normalisation simply means division by the total of the five coefficients. Probability ranges are then computed by summing the coefficients to produce 5 ranges (in two dimensions), $R_0 = 0$ to P_0 and $R_i = \sum_{j=0}^{i-1} P_j$ to $\sum_{j=0}^{i} P_j$, where $i = 1$ to 4. In three dimensions we similarly compute 7 probability ranges, $R_0 = 0$ to P_0 and $R_i = \sum_{j=0}^{i-1} P_j$ to $\sum_{j=0}^{i} P_j$, where $i = 1$ to 7. We then generate a random number between 0 and 1, and depending on the range which this number falls in, the current individual tumour cell under consideration will remain stationary (R_0) or move west (R_1), east (R_2), south (R_3) or north (R_4) in two dimensions, and additionally can move down (R_5) or up (R_6) in three dimensions. The larger a particular range, the greater the probability that the corresponding coefficient will be selected. Each tumour cell is therefore restricted to move to one of its four orthogonal neighbouring grid points (and additionally can move either up or down in three dimensions) or remain stationary at each time step.

All cells are given a unique identification number which is assigned as each new cell is produced (or is assigned initially for the first 50 cells). Each time step of the simulation involves firstly updating all of the cells positions (via the identification number i.e. the larger the identification number the later the update) then secondly updating the individual based processes for all the cells e.g. proliferation, death, mutation. Therefore cells are not updated simultaneously or in a left-to-right, top-to-bottom manner but as per the identification number. For the migration part of the update the identification method gives preference to cells which have smaller identification values (since they get to move before the others do) but since the cells are distributed all over the tumour this should not introduce any visible bias. Once the cells have moved the individual based processes are updated and this is done again per cell identification number but this time the

cells update as soon as a process occurs e.g. proliferation, this should avoid any conflicts for space.

5. HDC Simulation Results

Now that we have discussed the HDC model of tumour invasion in detail we shall use it to examine the impact of different microenvironments (e.g. homogeneous, heterogeneous tissue, low/high nutrient concentration) in combination with different mutation algorithms (i.e. linear or random). Most of the results will be presented in two dimensions, but in the final results section we consider tumour invasion in a random three dimensional tissue.

5.1. Invasion In Two Dimensions

The following simulations were carried out on a 400×400 grid, which is a discretisation of the unit square, $[0,1] \times [0,1]$, with a space step of $h = 0.0025$ and a time step of $k = 0.0005$. Note that with this choice of space step each square of grid is approximately the same area as a tumour cell i.e. $6.25 \times 10^{-6} cm^2$ (or $1.56 \times 10^{-8} cm^2$ as a volume, with cells of side $0.0025cm$). No flux boundary conditions were imposed on the square grid, restricting the tumour cells, MDE, MM and oxygen to within the grid. Initially, 50 tumour cells are centred around $(0.5, 0.5)$ with an assigned phenotype I, a random age between $0hrs - 16hrs$, the MDE concentration is zero throughout the domain ($m(x,y) = 0$) and the oxygen concentration is taken to be one ($c(x,y) = 1$). We consider the effects, upon tumour invasion, of three different MM initial distributions: (i) homogeneous ($f(x,y) = 1$), (ii) heterogeneous ($0 \leq f(x,y) \leq 1$), with f(x,y) being generated from a combination of sin and cos functions of the x and y directions and (iii) random ($0 \leq f(x,y) \leq 1$) in combination with two different mutation algorithms: (A) Linear and (B) Random. For clarity we shall label the resulting tumour cell distributions as A(i) homogeneous tumour, A(ii) heterogeneous tumour and A(iii) random tumour for the Linear mutation algorithm and similarly for the Random mutation algorithm but use the labels B(i), B(ii) and B(iii) for homogeneous, heterogeneous and random respectively. The non-dimensional parameter values used in all the following simulations are $d_n = 0.0005$, $d_m = 0.0005$, $d_c = 0.5$,$d_{c_{cell}} = 0.25$, $\rho = 0.01$, $\eta = 50$, $\kappa = 1$, $\sigma = 0$, $\nu = 0.5$, $\omega = 0.57$ and $\phi = 0.025$. We also take the phenotype mutation probability to be $P_{mutat} = 0.1$. Other values were considered and produced similar results but for shorter or longer times depending on whether the probability was larger or smaller.

Fig.3 shows the resulting tumour cell populations from simulations using either the linear or random mutation algorithms along with each of the three different initial MM distributions at $t = 200$ time units. What is immediately apparent is that all of the tumour cell distributions show a mainly dead central region with a thin dispersed proliferating boundary. What is also clear is that the tumours that grew in the homogeneous MM distribution, A(i) and B(i), have a more circular and symmetric morphology in contrast to those grown in the heterogeneous or random MM distributions, A(ii), A(iii), B(ii), and B(iii), which

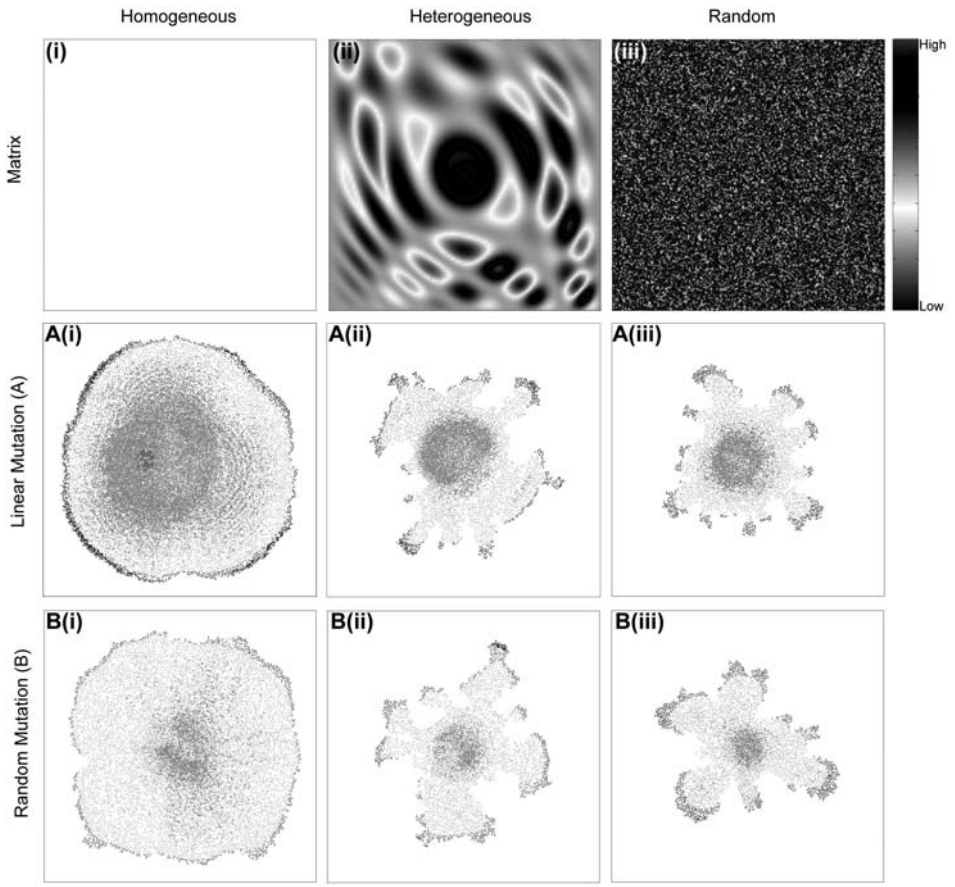

FIGURE 3. HDC tumour simulation results, at time $t = 200$ units, using three different initial MM distributions: (i) homogeneous, (ii) heterogeneous and (iii) random (upper row), using either the linear (middle row, A) or random (lower row, B) mutation algorithms. Density of MM is represented by colouration, as depicted in the color bar on the right. Cell colouration reflects dead cells (brown) or cell-cell adhesion (zero cell-cell adhesion = blue). For the linear mutation algorithm, blue also represents the most agressive phenotype (type IV, see Table 1). Simulation movies showing the growth of the tumour as well as the other three variables (i.e. MDE, MM and oxygen) for all six sets of results can be found on the accompanying DVD.

have a radically different geometry showing a more fingered morphology, with clusters of cells protruding from a central core.

For the linear mutation results, A(i)–A(iii), the fact that the resulting tumour cell populations consists of only one living cell type IV might not be surprising due to the linear nature of the mutations. However, it seems logical to assume that

it will be the most aggressive tumour cells that dominate the tumour population and they do so only at the boundary of the tumour. This is due to the fact that all the oxygen has been consumed within the main mass of the tumour, although, as can be seen in Fig.3 A(i), a small cluster of cells has survived in the centre of the tumour. This is partly because quiescent cells consume less oxygen and therefore allow for the diffusion of a little oxygen back into the centre of the tumour. Given more time, these cells will also die due to lack of oxygen. However, this does imply that even necrotic regions may still offer some potential for tumour cell survival (in the short term).

It is also perhaps understandable why tumour cells that were invading through an initially homogeneous distribution of MM, Fig.3 A(i) and B(i) produce more symmetric tumours. These homogeneous tumours also produced the largest number of individual cells, due to the combined effects of a faster invasion rate and subsequently access to empty space for proliferation leading to further invasion. The faster invasion is mainly driven by the cell-matrix interactions via haptotaxis, giving directed motion towards higher concentrations of MM. Since all of the cells on the boundary have no cell-cell adhesion dependence (denoted by the blue colour) they can exploit this gradient the most.

For the random mutation results, B(i)–B(iii), the resulting tumour morphologies are remarkably similair to those of the linear mutation, as is the distribution of cell adhesion (denoted by the cell colour). With the resulting tumour cell populations consisting of living cells with zero cell-cell adhesion all these occurring at the tumour perimeter. Due the random nature of the mutations this is somewhat surprising, as any of the 100 possible phenotypes can be randomly chosen. Given that all three linear mutation simulations, Fig.3 A(i)–A(iii), and all three random mutation simulations, Fig.3 B(i)–B(iii), use the same parameters, with the exception of the MM initial distributions, these results illustrate the importance of tumour cell microenvironmental interactions in aiding or hindering the migration of individual cells that define the tumour geometry.

These results are consistent with the experimental findings of Weaver [40], although they consider differences in MM tension as opposed to MM heterogeneity. But the effect is the same: by making the microenvironment more difficult (harsher) for the tumour to invade into, a fingered tumour displaying an invasive morphology results, Fig.3 A(ii), A(iii), B(ii) and B(iii). One of the major advantages of working with a computational model is the ability to keep track of all variables/paramters at all times. This allows us to examine the precise distribution of phenotypes for the random mutation results, Fig.3 B(i)–B(iii), as the tumour invaded each of the different MM distributions.

From Fig.4 we can see the evolution of the tumour phenotype distribution for each of the different MM distributions using the random mutation algorithm. We note that there are approximately 6 phenotypes in the homogenous tumour, 3 phenotypes in the heterogeneous tumour and 2 phenotypes in the random tumour that dominate the tumour population and survive for most of the simulation. Of these phenotypes all have a zero cell-cell adhesion value, most have a short proliferation

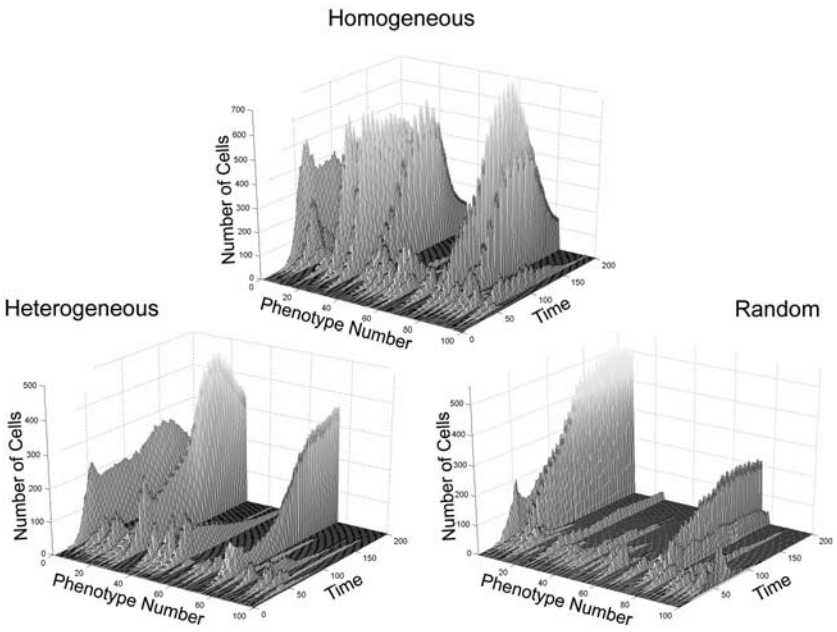

FIGURE 4. Phenotype distributions for each of the tumour populations in Fig.3 B(i)–B(iii), lower row, from simulations using the random mutation algorithm.

age, as well as high haptotaxis coefficients. Surprisingly, for each of the phenotypes that are selected, one in each population is the most aggressive phenotype, always being expressed by the largest fraction of cells in the tumour population, and always has the shortest proliferation age, highest haptotaxis coefficient, no cell-cell adhesion restrictions and, in contrast to the most aggressive type IV cells of the linear mutation algorithm, they mainly have low oxygen consumption rates. If we consider the random MM distribution, Fig.3(iii), as the harshest tissue microenvironment since cells will be receiving many conflicting migration signals from the rapidly varying MM density. Then not only do the more aggressive phenotypes get naturally selected but it would appear that the harsher the MM microenvironment the stronger the evolutionary pressure to select for the most aggressive clones i.e. MM heterogeneity enhances natural selection.

If the predictions made by these simulations are valid, they should be reproducible using different types of microenvironmental stress. Pennacchietti et al. [41] found very similar morphological and phenotypic changes when they grew tumour spheroids in either normoxic or hypoxic conditions. Fig.5 shows some of their results and the switch from the circular non-invasive morphology to the fingered invasive morphology can easily be seen. These results imply that starving

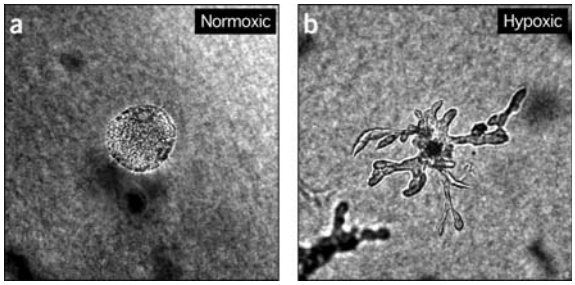

FIGURE 5. Experimental results adapted from Fig.6, Pennacchietti et al. [41], showing a tumour spheroid grown under normoxic and hypoxic conditions. Note the invasive morphology of the hypoxic tumour.

the tumour of oxygen will produce similar changes to that seen when changes in the MM distribution are made. Experimentally, the results shown in Fig.5 are obtained by placing pre-grown spheroids into two different oxygenated environments and allowing them to grow [41].

In order to try and replicate these results with the HDC model of invasion we will initially grow the tumour in an oxygen rich microenvironment (normoxic) then switch to a poorly oxygenated microenvironment (hypoxic), to ensure we only consider the influence of the oxygen concentration we will use the homogenous MM distribution, Fig.3(i), and since we are interested in how the oxygen will effect

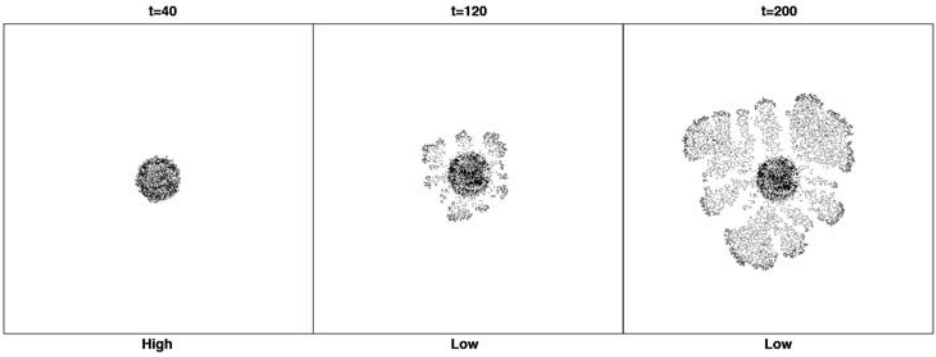

FIGURE 6. HDC tumour simulation results in a homogeneous MM (see Fig.3, top row) using the random mutation algorithm in combination with varying oxygen concentrations: From t=0-40, oxygen is kept at a high concentration and then t=41-200 oxygen is switched to a very low concentration. Note the switch in morphology between high and low oxygen concentrations. A simulation movie showing the growth of the tumour as well as the other three variables (i.e. MDE, MM and oxygen) for this result can be found on the accompanying DVD.

the genetic make up of the tumour we will use the random mutation algorithm. Fig.6 shows the resulting tumour cell distribution for three different snapshots in time. The oxygen rich tumour at $t = 40$ has a well defined circular non-invasive morphology with a mixture of many different phenotypes (seen by the different cell colours which represent the adhesion value of each cell, see Table 1). It is interesting to note that even though the mutations are random, and there is no real evolutionary pressure due to the high levels of oxygen, the tumour naturally sorts the cells with the lowest cell-cell adhesion to the boundary and those with higher adhesion are in the centre. As soon as the oxygen level is switched the morphology changes with a dead inner core of cells surrounded by invasive fingers ($t = 120$) that grow as time evolves ($t = 200$) i.e. an invasive morphology.

These results qualitatively match what is seen in the experimental situation (Fig.5). But they also give an extra level of detail that can only be seen by examining the phenotype distribution. Fig.7 shows how the numbers of the different phenotypes in the tumour population evolve in time. In the normoxic microenvironment ($t = 0 - 40$) most of the 100 phenotypes are present at similar numbers. However, almost as soon as the switch to hypoxic conditions occurs ($t = 41 - 200$) we see the number of phenotypes present drops, leaving only three to dominate for the rest of the simulation. By examining each of these dominant phenotypes we find that, just as under the harsh MM conditions (cf. Fig. 4), each of them have a zero cell-cell adhesion value, a short proliferation age, as well as high haptotaxis coefficients and of course low oxygen consumption rates. Therefore, we again see that under harsh microenvironmental conditions, an increase in the evolutionary pressure occurs causing selection in the resulting tumour population for the most aggressive clones that result in a tumour with an invasive morphology.

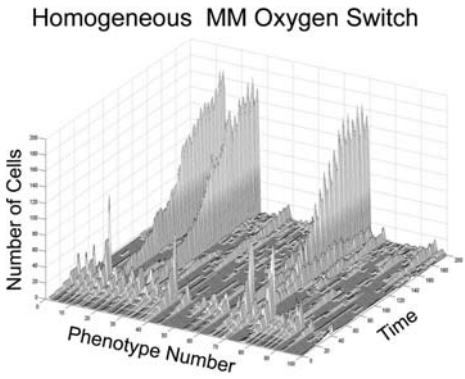

FIGURE 7. Phenotype distribution for the tumour population in Fig.6

5.2. Invasion In Three Dimensions

Whilst a model of a two dimensional section through a three dimensional tumour can give a great deal of insight, as we have seen above, we are aware of its limitations. In particular, cell migration is greatly restricted in two dimensions, as is cell-cell adhesion both of which are central to the invasive process. We therefore extended the model to three dimensions, which is fairly straightforward to do as the parameters and variables in the model do not change, the only real change that occurs is that we switch to using the movement probabilities given in Eqs.(7)–(8) as well as a three dimensional representation of the continuous variables in system Eq.(2).

The following simulation was carried out on a $160 \times 160 \times 160$ grid, which is a discretisation of the unit cube, $[0,1] \times [0,1] \times [0,1]$, with a space step of $h = 0.00625$ and a time step of $k = 0.0005$. Note that with this choice of space step this cube of tissue could possibly contain well over four million tumour cells. In comparison to the two dimensional case of at most 40000 cells, the computational magnitude of working in three dimensions is brought sharply into focus. No flux boundary conditions were imposed on the cubed grid, restricting the tumour cells, MDE, MM and oxygen to within the grid. Initially, 50 tumour cells are centred around $(0.5, 0.5, 0.5)$ with an assigned phenotype I, a random age between $0hrs - 16hrs$, the MDE concentration is zero throughout the domain ($m(x,y,z) = 0$) and the oxygen concentration is taken to be one ($c(x,y,z) = 1$). We will specifically focus on the effect that a random ($0 \leq f(x,y,z) \leq 1$) initial MM distribution has on the growing tumour in three spatial dimensions using the linear mutation algorithm. for both speed and simplicity.

Fig.8A shows the tumour almost filling the entire volume after 200 time units. Another issue when dealing with three dimensional results is being able to visualise them suitably [18]. In order to see what is actually happening within this tumour volume I only visualise two orthogonal slices (Fig.8B-D). Perhaps unsurprisingly we see a very similair fingered morphology to that obtained in the equivalent two dimensional results (Fig.3A(iii)). This fingered morphology is seen no matter how the tumour volume is sliced and therefore further strengthens the two dimensional results that show the emergence of an invasive phenotype under harsh microenvironmental conditions. The phenotypes that make up this cube of tumour tissue have a similar distribution to that seen in the two dimensional case, where the bulk of the outer boundary is dominated by the most aggressive type IV cells and the bulk of the inner core is dead cells.

6. Conclusions

In this chapter we examined the effects of the tumour microenvironment upon both the morphology and genetic makeup of a growing invading tumour. By using a combination of different microenvironments (e.g. homogeneous, heterogeneous tissue, low/high oxygen concentration) with different mutation algorithms (i.e.